Universitat de les Illes Balears

Facultat de Ciencies

Memòria del Treball de Fi de Grau

A model of disordered wire with Anderson localization

Cristian Estarellas Martin

Grau de Física

Any acadèmic 2014-15

DNI de l'alumne: 43224554X

Treball tutelat per Llorenç Serra Crespí
Departament de Física

Paraules clau del treball:
Quantum wires, scattering theory, Anderson localization

Agradecimientos

En primer lugar me gustaría agradecer a mi tutor, Llorenç Serra, por la ayuda que me ha ofrecido, sus consejos y su apoyo en todo momento que me ha permitido mejorar en el ámbito científico y en el estudio de la nanociencia y la mecánica cuántica. También agradecer a mi hermana, por su apoyo, sus consejos y por comprenderme como científica (*La vida es dura, y verde la verdura*). Agradecer a mis padres y a mis abuelos por preocuparse en las largas noches de estudio en la Riera y por los ánimos en los días de cansancio. A mis amigos por la paciencia que han tenido al aguantarme en los días de estrés y a Lorena por darme fuerzas y dibujarme una sonrisa en mi rostro en los momentos más complicados.

Contents

Chapter 1

Introduction

Nanotechnology can be defined as the study of microstructures of materials using electron microscopy and the growth and characterization of thin films, or a bottom-up approach in materials synthesis and fabrication, such as self-assembly or biomineralization to form hierarchical structures like abalone shell. Even it can mean something startlingly new, such as miniature submarines in the bloodstream, smart self-replication nanorobots monitoring our body, space elevators made of nanotubes and the colonization of the space. Since these examples are different statements that people working in nanotechnology use to define the field, it proves the extensive spectrum of research [1].

In general, nanotechnology can be understood as a technology of design, fabrication and application, as well as fundamental understanding of physical properties and phenomena of nanostructures and nanomaterials. But the study of materials in the nanometer scale has been traced for centuries, for example the study of biological systems and the engineering of many materials such as colloidal dispersions, metallic quantum dots, and catalysts have been in the nanometer regime [1].

The current fever of nanotechnology is partially due to the shrinking of devices in the semiconductor industry. As the Moore's law says [2], the technology tends to shrink arriving at nanometer scale which is the working scale of the nanoscience. Currently, the typical dimension involves from subnanometer to several hundreds of nanometers.

A nanometer (nm) is one billionth of a meter, 10^{-9} m, approximately the length equivalent to 10 hydrogen or 5 silicon atoms aligned in line. The figure 1.2 shows an example of the position of nanodevices in the scale compared with other known systems.

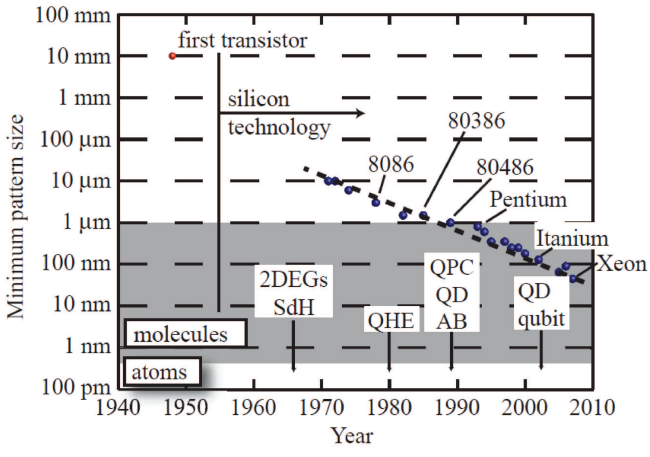

Figure 1.1: Sketch of Moore's law in the evolution.

These small structures or small-materials have different physical properties because of quantum physics important role.

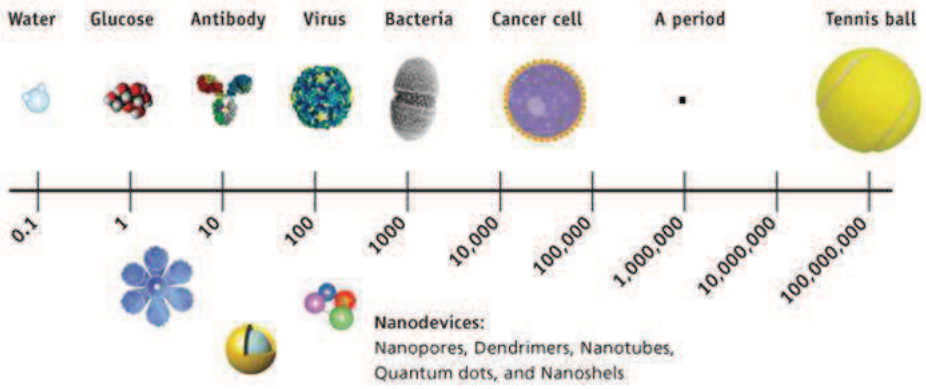

Figure 1.2: Scale comparison of the nanodevices.

Many technologies have been explored to fabricate nanostructures and nanomaterials [1]. These technical approaches can be grouped in several ways. One of them is to group the techniques according to the form of products:

- Nanoparticles (zero-dimensional nanostructure) by means of colloidal processing, flame combustion and phase segregation.
- Nanorods or nanowires (one-dimensional nanostructure) by template-based electroplating, solution-liquid-solid growth (SLS), and spontaneous anisotropic growth.
- Thin films (two-dimensional nanostructure) by molecular beam epitaxy (MBE) and atomic layer deposition (ALD).
- Nanostructured bulk materials, for example, photonic badgap crystals by self assembly of nanosized particles.

1.1 Nanowires

Quantum wire is known as one-dimensional nanostructure formed by many techniques such as spontaneous growth, template-based synthesis, electrospinning and lithography. The structure is characterised by a diameter not exceeding a few hundred nanometers (see Figure 1.3).

This kind of nanostructure has many applications in different sectors such as energy, environment or electronics. There are different utilities as possible filters compost by nanowires to kill bacteria in water. In addition, researchers at Nies Bohr Institute have determined that sunlight can be concentrated in nanowires so it can be applied in solar cells, transforming more solar energy in electricity [3]. Evidently, this type of structure can also be used to fabricate transistors and devices improving their conductances and the information transmitted.

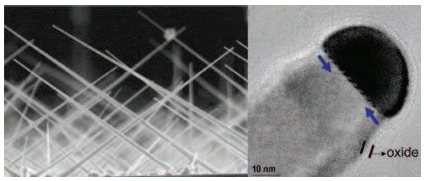

Figure 1.3: Photography of nanowires and an enlargement of one of them with 10 nm of scale.

1.1.1 Wave propagation in quasi-one-dimensional wires

Considering an ideal quantum wire, the wave function can be separated as shown in the equation (1.1), formed by a wave plane function in the longitudinal direction (x) where L is a normalization length and $\chi_n(y)$, that are quantized states normal to the wire direction called *transverse modes*. The energy from the system is expressed with the equation (1.2) where E_n is the energy obtained by the transverse mode n [4].

$$\psi_{n\boldsymbol{k}}(\boldsymbol{r}) = \chi_n(y)\frac{1}{\sqrt{L}}e^{ik_x x} \ , \tag{1.1}$$

$$E_n(k_x) = E_n + \frac{\hbar^2 k_x^2}{2m^*} \ . \tag{1.2}$$

These results can be determined from the split of the Hamiltonian into two parts. One corresponding to the longitudinal direction (1.3) and another one corresponding to the normal direction (1.4). The last one contains the potential that determined the transverse modes. In this research, the potential used is an infinite square well. For this reason the wave function becomes the equation (1.5) and the energy is (1.6), where W is the width of the wire and k_n the transversal mode.

$$H_x = -\frac{\hbar^2}{2m^*}\frac{\partial^2}{\partial x^2} \ , \tag{1.3}$$

$$H_y = -\frac{\hbar^2}{2m^*}\frac{\partial^2}{\partial y^2} + V(x;y) \ , \tag{1.4}$$

$$\Psi_n(x,y) = (a_n e^{ik_n x} + b_n e^{-ik_n x})\sin\left[\left(\frac{n\pi}{W}\right)y\right] \ , \tag{1.5}$$

$$E_n(k_n) = \frac{\hbar^2\pi^2}{2m^*W^2}n^2 + \frac{\hbar^2 k_n^2}{2m^*} \ . \tag{1.6}$$

1.1.2 Conductance

In a scattering process the electron can be reflected or transmitted. This effect has an important influence into the current, that at low temperature is written as the equation (1.7), where g_s is the degeneracy, e the charge from the electron, $T_n = |t_n|^2$ is the transmission by a determined mode n and the voltage V_{SD} appears due to the difference potential between the terminals of the wire extremes. By the Ohm's law, the current is proportional to the voltage $I = GV$, where G is the conductance [4].

$$I = g_s\frac{|e|^2}{h}V_{SD}\sum_n T_n(E) \ . \tag{1.7}$$

The quantum conductance (1.8) at low temperature is obtained associating the Ohm's law with the current (1.7). Particularly, the model is restricted to low energies, in order to use only one mode. This fact simplifies the scatterer problem because there are no possible couplings between transversal modes or more of one transmission coefficient per scatter. As a result, the conductance has the simple form of equation (1.9).

$$G = g_s \frac{e^2}{h} \sum_n T_n(E) \ , \tag{1.8}$$

$$G = g_s \frac{e^2}{h} T(E) = G_o T(E) \ . \tag{1.9}$$

In an ideal quantum wire, the conductance is quantized as $G = G_o N$ depending on the number of occupied modes N where the quantum conductance is $G_o = g_s e^2/h$. It is a curious phenomenon which implies the existence of an intrinsic resistance into a perfect nanowire. Nevertheless, if the wire has impurities that are treated as scatterers, the conductance will be determined by the equation (1.9). In the simile of Ohm's law, this conductance is inversely proportional to the length of the wire. But if the impurities are randomly dispersed by the wire, the linear behaviour can be different for a significant number of scatters. This phenomenon was studied by Anderson.

1.2 The Anderson localization

Anderson was the first one to suggest the possibility of electron localization within a semiconductor due to the degree of randomness when the number of impurities was sufficiently large. In this way, the absence of diffusion of waves stands out in a disordered medium [5]. The Anderson's localization phenomenon appears in the transport of electromagnetic waves, acoustic waves, quantum waves, or spin waves.

Figure 1.4: Philip Warren Anderson (born December 13, 1923)

From the contributions of Anderson, the statistical properties of wave transport through disordered media has been studied, such as the conductance behaviour in a nanowire. In this kind of one-dimensional system there are three different transport regime: Ballistic, Diffusive and Localized. These regimes differ in their conductance probabilistic distributions $P(G)$ and there are several studies about the behaviour of this distribution in each regime and the transition between them [6–8].

In general, a wire with disordered impurities with a determined length L implies that the conductance is a random variable characterized by a certain probability distribution $P_{L,\gamma}(G)$ because of the infinite ways that the impurities can be distributed. The probability distribution depends on the length L and the parameter γ, known as Lyapunov exponent, that has the relation with the conductance and wire length shown in the equation (1.10), where the value of N is the number of occupied modes which will be $N = 1$ for the rest of the work. Consequently, the distribution $P_{L,\gamma}(G)$ changes strongly with L [9].

The localization length is obtained from the inverse of the Lyapunov exponent ($\ell = \gamma^{-1}$). With this parameter it is possible to distinguish the localized and metallic (ballistic) regimes which implies different limits in the equation (1.11).

$$\gamma = \frac{1}{L} log\left(1 + \frac{G_o}{G} - \frac{1}{N}\right) , \tag{1.10}$$

$$G = \frac{G_o}{e^{\gamma L}} . \tag{1.11}$$

- **Localized regime**,
  This regime appears when $L \gg \ell$ and γ is normally distributed. In this case the conductance from the equation (1.11) with one occupied mode is given by the non-Ohmic relation

$$G = G_o e^{-\gamma L} . \tag{1.12}$$

- **Metallic regime**,
  The metallic regime emerges when $L \ll \ell$, then the conductance is normally distributed. The behaviour conductance is the same in the semiclassical description, inversely proportional to the length.

$$G = \frac{G_o}{\beta L + 1} . \tag{1.13}$$

The diffusive regime is the transition between the localized and metallic regimes and in this situation neither the conductance nor the Lyapunov exponent have a Gaussian distribution.

1.3 Motivation

This study is focused on the transmission properties in a wire composed by several ideal nanowires linked by vertexes randomly distributed. Therefore, the conductance distribution, the Lyapunov's exponent and the resistance will be determined in three regions (metallic, diffusive and localized) verifying the Anderson localization theory. The randomness of the system is in the lengths of the linear segments and in the vertices, particularly in the angles.

If the variation of the random parameters are very small, for a several number of vertexes, the system can be seen as an almost "perfect nanowire", as it is observed in Figure 1.5.

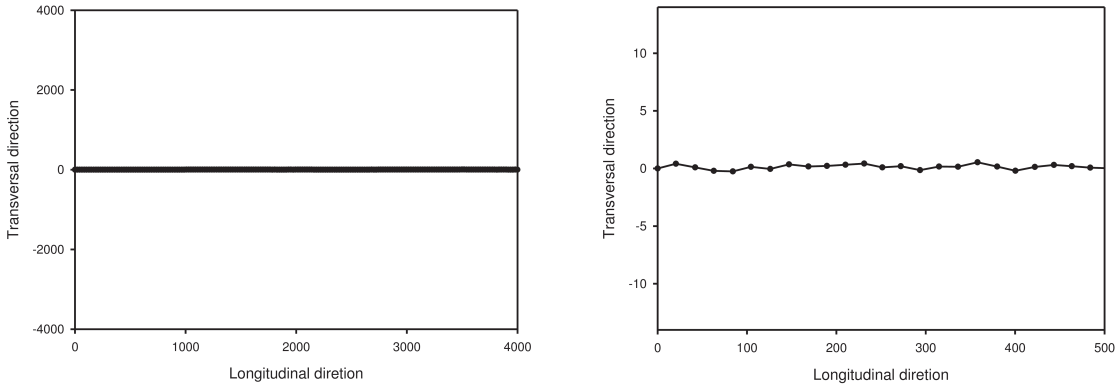

(a) Sketch of the complete system with several number of disordered impurities.

(b) Sketch of a system a few disordered impurities.

Figure 1.5: Simulation of the system that seems a perfect wire (a) as a result of the huge length compared with the transversal variation that can be observe in the simulation (b). This one is an enlargement of the first one.

The vertex in a quantum wire can have a bend form made by lithographic techniques, that has been a subject of interest [10–13]. To describe a bend we need two dimensions, but in this work it has been used an analytical approximation to obtain one-dimensional problem transforming the bend into a square well potential.

Each vertex is treated as a scatterer in a random position linked by ideal wires with random length. In order to determine the conductance it is necessary to know the transmission through the system calculated by scattering theory.

Chapter 2

Scatter of a vertex

Understanding the vertex is the aim of this chapter. Hence, the scattering matrix of the vertex and the effect of consecutive vertexes will be determined. This impurity is treated as a quantum wire with a circular bend, so the general problem has two dimensions. The scattering matrix allows to consider the circular bend as a scatter point, that is, a vertex. This subject was studied by Sols and Macucci [11] obtaining equations with numerical solutions. However, this work is focused on the studies of Sprung, Martorell and Wu [12] and Jensen and Koppe [14] that using some approximations achieve an equation which can be resolved analytically.

2.1 Scattering matrix of a circular bend

The problem can be separated in three parts as shown in Figure 2.1. Two of them (I and III) are treated as ideal wires using the theory mentioned above with the equations (1.5) and (1.6). Specifically, the equation used is (2.1) where $R = r_o + W$ is the over radius. For a given energy it is possible to determine the transversal mode with the equation (2.2) where the system energy is into $\kappa = 2m^*E/\hbar^2$.

$$\Psi_{I,III}(x,r) = (ae^{\pm \imath k_n x} + be^{\mp \imath k_n x}) \sin\left[\left(\frac{n\pi}{W}\right)(r-R)\right] \ , \tag{2.1}$$

$$k_n = \kappa - \left(\frac{n\pi}{W}\right)^2 \ . \tag{2.2}$$

For the region II it is necessary to use the Schrödinger equation in polar coordinates (r,θ) (2.3) which is transformed in (2.5) using the Jensen and Koppe ansatz (2.4) [14].

$$\frac{\partial^2\psi}{\partial r^2} + \frac{1}{r}\frac{\partial\psi}{\partial r} + \frac{1}{r^2}\frac{\partial^2\psi}{\partial\theta^2} + \kappa^2\psi = 0 \ , \tag{2.3}$$

$$\psi(r,\theta) = \frac{1}{\sqrt{r}}\chi(r,\theta) \ , \tag{2.4}$$

$$\frac{\partial^2\chi}{\partial r^2} + \frac{1}{4r^2}\chi + \frac{1}{r^2}\frac{\partial^2\chi}{\partial\theta^2} + \kappa^2\chi = 0 \ , \tag{2.5}$$

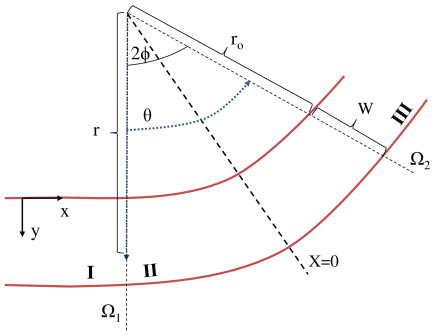

Figure 2.1: Sketch of a quantum wire with circular bend. It is organized in three regions separated by the outlines Ω_1 and Ω_2, where I and III are ideal nanowires and the region III is the circular bend with an angle 2θ and inner radius r_o.

There are crucial approximations used by Sprung, Martorell and Wu [12] to resolve the equation (2.5). The first one and very restrictive is to replace r^2 by an average value $\overline{R}^2$ (2.6).

$$\frac{1}{\overline{R}^2} \equiv \frac{1}{W}\int_R^{R+W} dr = \frac{1}{R(R+W)} \; . \tag{2.6}$$

With this approximation equation (2.5) becomes (2.9), where $x = \overline{R}\theta$. The new form has a separable solution (2.8) formed by $\Phi_n(x)$, the longitudinal motion through the bend.

$$\frac{\partial^2\chi}{\partial r^2} + \frac{\partial^2\chi}{\partial x^2} + \left(\frac{1}{4\overline{R}^2} + \kappa^2\right)\chi = 0 \; , \tag{2.7}$$

$$\psi_n(r,\theta) = \frac{1}{\sqrt{r}}\Phi_n(x)\sin\left[\left(\frac{n\pi}{W}\right)(r-R)\right] \; . \tag{2.8}$$

The second approximation that is taken into account is to consider the value "$1/\sqrt{r}$" as a constant. In this way the longitudinal solution is used to solve the equation (2.9).

$$\frac{\partial^2\Phi_n}{\partial x^2} + \left(p_n^2 + \frac{1}{4\overline{R}^2}\right)\Phi_n = 0 \; . \tag{2.9}$$

These approximations replace the motion in the circular bend by the motion in a straight section with a finite square well potential of depth $V = (\hbar^2/2m^*)(1/2\overline{R})^2$ into the limits $x = \pm\overline{R}\Theta = \pm\alpha$. The function (2.10) shows the analytical wave function in the system of a wire with circular bend region.

$$\Psi_n(x,r) = \begin{cases} \psi_{I,n} = (a_{n,l}e^{\imath p_n x} + b_{n,l}e^{-\imath p_n x})\sin\left[\left(\frac{n\pi}{W}\right)(r-r_o)\right] , & \text{if } x < -\alpha \\ \psi_{II,n} = \frac{1}{\sqrt{r_o}}(c_n e^{\imath q_n x} + d_n e^{-\imath q_n x})\sin\left[\left(\frac{n\pi}{W}\right)(r-r_o)\right] , & \text{if } -\alpha < x < \alpha \\ \psi_{III,n} = (b_{n,r}e^{\imath p_n x} + a_{n,r}e^{-\imath p_n x})\sin\left[\left(\frac{n\pi}{W}\right)(r-r_o)\right] . & \text{if } x > \alpha \end{cases} \tag{2.10}$$

Where the mode wave number used in the circular region (q_n) has the relation $q_n^2 = p_n^2 + 1/4\overline{R}^2$ by the expression (2.9). In this way, the two-dimensional problem has been transformed into one-dimensional, as shown in Figure 2.2.

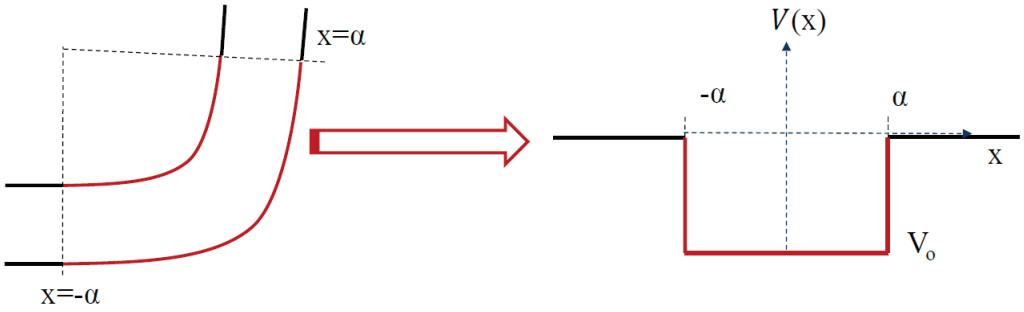

Figure 2.2: Circular bend sketch on the left that is transformed in the attractive potential with the potential $V_0 = \hbar^2/(4m^*\overline{R}^2)$

The global wave function has to be continuous as well as its first derivative and therefore these conditions have to be satisfied at the interface between different regions. For the first interface corresponding to $x = -\alpha$ the conditions (2.11) are applied and for the second interface the conditions (2.12) with $x = \alpha$ are used.

$$\psi_I|_{x=-\alpha} = \psi_{II}|_{x=-\alpha} \quad \text{and} \quad \left.\frac{\partial\psi_I}{\partial x}\right|_{x=-\alpha} = \left.\frac{\partial\psi_{II}}{\partial x}\right|_{x=-\alpha} , \tag{2.11}$$

$$\psi_{II}|_{x=\alpha} = \psi_{III}|_{x=\alpha} \quad \text{and} \quad \left.\frac{\partial\psi_{II}}{\partial x}\right|_{x=\alpha} = \left.\frac{\partial\psi_{III}}{\partial x}\right|_{x=\alpha} . \tag{2.12}$$

These conditions lead to the scattering matrix of the system. As it has been commented, this project is realized in the limit at low energies and a small enough width of the nanowire to consider only the first mode. For this reason, the scattering matrix will have four components with the following structure (2.13), that connects the output and input coefficients (b_l, b_r, a_l, a_r, respectively) of the longitudinal function.

$$\begin{pmatrix} b_l \\ b_r \end{pmatrix} = \begin{pmatrix} r & t \\ t' & r' \end{pmatrix} \begin{pmatrix} a_l \\ a_r \end{pmatrix} . \tag{2.13}$$

The eigenenergy for the first transversal mode is $\varepsilon_1 = \hbar^2\pi^2/(2m^*W^2)$. Knowing the energies and the potential it is possible to write the wave number p and q as (2.14) and (2.15). The scattering coefficients (2.16-2.17) depend on the energy of the system (E) and the angle and average radius of the circular bend ($\theta, \overline{R}$), that are concealed into the modes p, q and the value of α. It is important to emphasize the fact that the transmission and reflection coefficients are the same for left and right incidences, $t = t'$, $r = r'$, due to the symmetry of the bend.

$$p = \sqrt{\frac{2m^*}{\hbar^2}(E - \varepsilon_1)} , \tag{2.14}$$

$$q = \sqrt{\frac{2m^*}{\hbar^2}(E - \varepsilon_1 - V_0)} , \tag{2.15}$$

$$t = \frac{4pq}{(p+q)^2 e^{2\imath(p-q)\alpha} - (p-q)^2 e^{2\imath(p+q)\alpha}} , \tag{2.16}$$

$$r = \frac{2\imath(p-q)(p+q)\sin(2q\alpha)}{(p+q)^2 e^{2\imath(p-q)\alpha} - (p-q)^2 e^{2\imath(p+q)\alpha}} . \tag{2.17}$$

Where α was previously defined as $\alpha = \bar{R}\theta$.

2.2 Process with consecutive vertexes

Considering the vertex as an impurity with the scattering matrix determined in the previous section, it gives a relation between input and output coefficients knowing the transmission and reflection caused by the scatterer. This section treats the relation between the coefficients of the longitudinal function when there are three consecutive vertexes (see Figure 2.3).

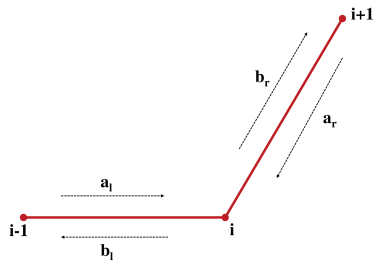

Figure 2.3: Sketch of three consecutive vertexes with input and output coefficients in each quantum wire.

The coefficient labelling is structured with a superindex indicating the number of the vertex and the subindex referring to the side of the vertex. Wave function in quantum wire can be written depending on the vertex used (2.18). This fact implies the relation (2.19) and (2.20). The amplitudes differ by a phase that appears due to the assumption of two different reference points.

$$\Phi_{(i\to i+1)} = a_r^{(i)} e^{-\imath p(x-x_i)} + b_r^{(i)} e^{\imath p(x-x_i)} = a_l^{(i+1)} e^{\imath p(x-x_{i+1})} + b_l^{(i+1)} e^{-\imath p(x-x_{i+1})} \,, \tag{2.18}$$

$$b_l^{(i)} = a_r^{(i-1)} e^{-\imath p(x_i-x_{i-1})} \,, \tag{2.19}$$

$$b_r^{(i)} = a_l^{(i+1)} e^{-\imath p(x_{i+1}-x_i)} \,. \tag{2.20}$$

To determine the output and input coefficients in a chain formed by vertices the equations (2.13, 2.19 and 2.20) are used for each vertex giving a system with $4N$ unknown quantities and $4N$ equations, where N is the number of vertices.

Chapter 3

System of many impurities

The Anderson localization phenomenon appears when the system has a large size with several impurities randomly distributed. The aim of this chapter is to describe the physical problem through a system of equations which determines the scattering amplitudes useful to know quantities such as the conductance, the resistance and Lyapunov exponent and therefore the disordered system behaviour will be known. On top of that, random variables are defined and the relation between them and the vertex is explained.

In addition, the generation of random number is created by a Fortran subroutine which is the programming code used to compute the physical problem.

3.1 Random variables

The system is made of two components (see Figure 3.1). The first one, ideal quantum wire of random length which has the expression (3.1), where l_0 is the standard length adding a small variation l'. In particular, this added length is always the 10% of l_0. The second one, the vertex with a random angle regarding the horizontal axis (3.2), where θ_0 is the absolute value of the maximum deviation angle. The randomness in this variables appears in the random number ζ that spans from 0 until 1. Global length of the system is connected with the number of vertices N_v and the constant l_0 by the relation $L \approx N_v l_0$.

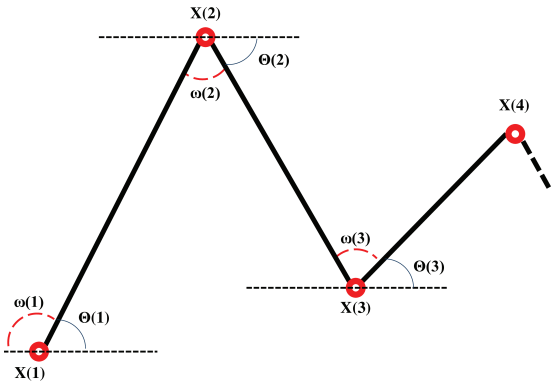

Figure 3.1: Sketch of the system built by random vertices and ideal wires of random length.

$$l = l_0 + \zeta l' \,, \tag{3.1}$$

$$\theta = \theta_0(1 - 2\zeta) \,. \tag{3.2}$$

As it is observed in Figure 3.1, the vertex i has a random position $x(i)$ which depends on the angle θ (3.2) and length l (3.1) (random values for each vertex). The position is determined by the equation (3.3) considering the first position $x(1) = 0$. In order to plot the sketch in a two dimensional graphic with euclidean coordinates, as the Figure 1.5, the cartessian position of a vertex i is described by equations (3.4) and (3.5).

$$x(i) = x(i-1) + l \ , \tag{3.3}$$

$$x_i = [x(i) - x(i-1)] \cos\theta(i-1) \ , \tag{3.4}$$

$$y_i = [x(i) - x(i-1)] \sin\theta(i-1) \ . \tag{3.5}$$

Scattering matrix for a vertex uses the smallest angle between its sides (ω) (see Figure 3.1), whereas the angle used to build the system is θ. Hence, the relation between both angles for the first vertex is determined by the equation (3.6) and the rest of them follow the equation (3.7).

$$\omega(1) = \pi - \theta(1) \ , \tag{3.6}$$

$$\omega(i) = \theta(i-1) + \pi - \theta(i) \ . \tag{3.7}$$

3.2 System of equations

The physical structure can be split in three regions. One of them is characterized by the fact that each vertex is surrounded by two of them. If the system has N vertexes, this region is formed by $N-2$ of them. Each scatterer defines one system of equations (3.8) formed by equations (2.13, 2.19, 2.20) that depends on the random variables calculated and the energy used.

$$\left.\begin{aligned} b_l^{(i)} - r a_l^{(i)} - t a_r^{(i)} &= 0 \\ b_r^{(i)} - t a_l^{(i)} - r a_r^{(i)} &= 0 \\ b_l^{(i)} - a_r^{(i-1)} e^{-\imath p(x_i - x_{i-1})} &= 0 \\ b_r^{(i)} - a_l^{(i+1)} e^{-\imath p(x_{i+1} - x_i)} &= 0 \end{aligned}\right\} \ . \tag{3.8}$$

The rest of regions are the first and the last vertex. These cases have some restriction because of initial conditions of the system which are the values of the amplitude input coefficient for the first vertex, $a_l^{(1)} = 1$, and for the last vertex the right input coefficient $a_r^{(N)} = 0$. This conditions say that plane waves only come from the right. In addition, taking into account that first and last impurity has only one neighbor vertex there is one equation less.

As a result, the system of the equations (3.9) belongs to the vertex $i = 1$ and the equation (2.19) is eliminated. The system (3.10) belongs to the vertex $i = N$ and does not contain the equation (2.20).

$$\left.\begin{aligned} b_l^{(1)} - r a_l^{(1)} - t a_r^{(1)} &= 0 \\ b_r^{(1)} - t a_l^{(1)} - r a_r^{(1)} &= 0 \\ b_r^{(1)} - a_l^{(2)} e^{-\imath p(x_2 - x_1)} &= 0 \end{aligned}\right\} , \tag{3.9}$$

$$\left.\begin{aligned} b_l^{(N)} - r a_l^{(N)} - t a_r^{(N)} &= 0 \\ b_r^{(N)} - t a_l^{(N)} - r a_r^{(N)} &= 0 \\ b_l^{(N)} - a_r^{(N-1)} e^{-\imath p(x_N - x_{N-1})} &= 0 \end{aligned}\right\} . \tag{3.10}$$

The global structure of N impurities is formed by the combination of the system corresponding to each vertex. Consequently, the general system to resolve is not homogeneous and contains $4N - 2$ equations and $4N - 2$ unknown quantities (3.11).

$$\left(\begin{array}{c} M \\ (4N-2) \times (4N-2) \end{array}\right) \begin{pmatrix} b_l^{(1)} \\ b_r^{(1)} \\ a_l^{(1)} \\ a_r^{(1)} \\ b_l^{(2)} \\ \vdots \\ a_l^{(N)} \\ a_r^{(N)} \end{pmatrix} = \begin{pmatrix} 0 \\ 0 \\ 1 \\ 0 \\ 0 \\ \vdots \\ 0 \\ 0 \end{pmatrix} . \tag{3.11}$$

Chapter 4

Anderson localization

In this section, Anderson localization properties are studied for the analyzed system. The aim is to know the features of the nanowire such as the conductance (G), resistance (ρ) and the Lyapunove exponent (γ). It is a statistical problem, then it is necessary a large enough number of iterations to determine the average values of the wire characteristic due to the randomness of its impurities.

The system is defined by three important parameters such as the average length (l_o) of the equation (3.1), the angle deviation (θ_o) shown in the equation (3.2) explained in the section below and the energy (E) higher than the energy necessary to activate the first transversal mode, $\varepsilon_1 = \hbar^2\pi^2/(2md^2)$. In this work, the radius of the circular bend is a constant value, but it could be considered another random parameter. This fact would imply the variation of the depth of the square well potential making stronger the vertex scatter.

Conductance written in the Landauer equation (1.9) depends on the transmission coefficient (4.1) and therefore the resistivity is its inverse, Eq. (4.3), where ρ_o is the quantum resistivity. Another important parameter for this study is the Lyapunov exponent (1.10) that provides the localization length (ℓ) whose value classifies the structure, as it has been explained above, in three regions: metallic, diffusive and localized.

$$\mathcal{T}(E) = \frac{|b_r^{(N)}|^2}{|a_l^{(1)}|^2} = |b_r^{(N)}|^2 \,, \tag{4.1}$$

$$G = G_o|b_r^{(N)}|^2 \,, \tag{4.2}$$

$$\rho = \frac{1}{G} = \rho_o \frac{1}{|b_r^{(N)}|^2} \,. \tag{4.3}$$

The length unity is scaled to obtain general results. For this reason, the width of the nanowire d is used as unity of the length. For instance, if the localization length is $\ell = 120d$, with one width $d = 1$nm or $d = 2$nm the corresponding result would be $\ell = 120$nm or $\ell = 120 \times 2\text{nm} = 240$nm. The unit of energy is $\hbar^2/(2m^*d^2)$.

4.1 Main results

In a particular case, we checked the behaviour of the nanowire properties in the three regions explained bellow. The next results correspond to the system with $l_0 = 20d$, $E = 4.94$, $\theta_0 = 1$. The use of this specific angle increases the square well length, increasing the scattering in the vertex. This effect reduces the computer power load.

4.1.1 Lyapunov exponent

The classification of the system can be known with the Lyapunov exponent. This quantity is useful because its inverse is the localization length, that is compared with the global length of the wire as it was commented in section 1.2. In particular, its value is determined in the localized region where γ has a normal distribution.

Histograms in Figure 4.1 show the parameter behaviour for the different regions. The important case is the last one, corresponding to the localized domain. The number of vertexes used is $N_v = 200$. Remarkably, for a higher number N_v the expected value is the same. Then, the localization length is independent of the number of impurities.

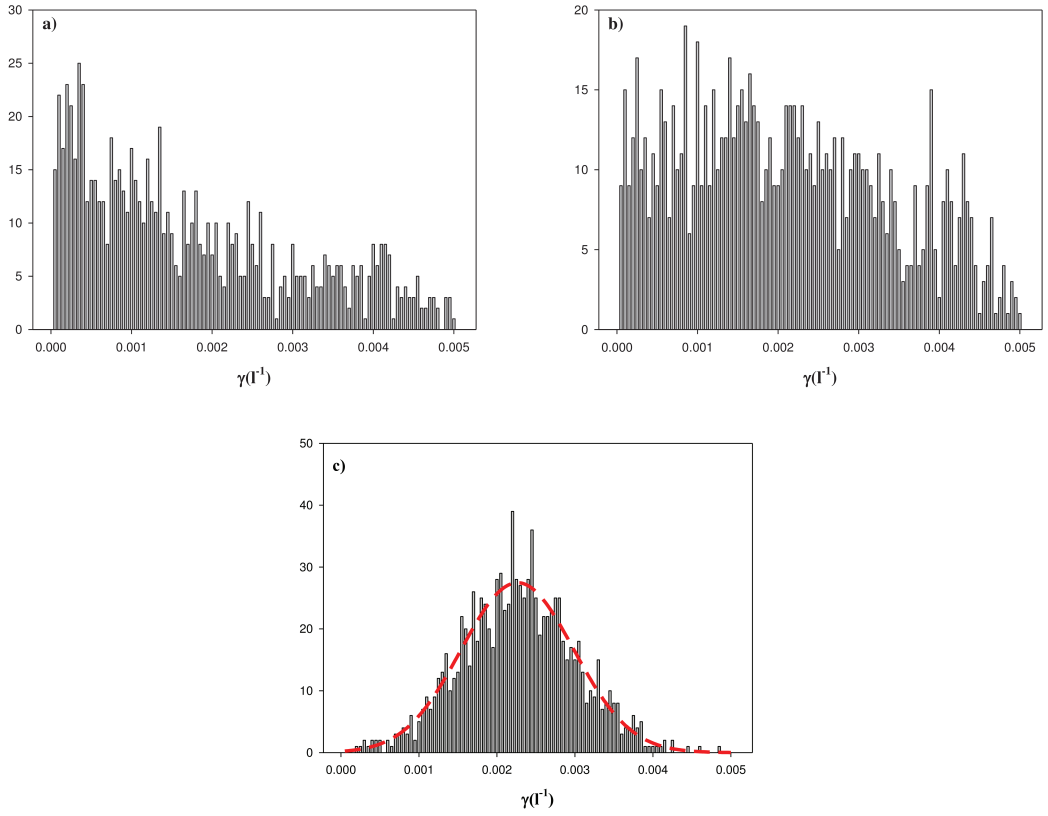

Figure 4.1: Histograms of the Lyapunov exponent in the three type of region: metallic (a), diffusive (b) and localized (c). The parameters used are $l_0 = 20d$, $\theta_0 = 1$, $E = 4.94$ and $N_v = 200$. The dashed red line in (c) shows the gaussian distribution.

For the last case of Figure 4.1, the expected value is $\langle\gamma\rangle = 2.2725 \cdot 10^{-3} d^{-1}$ providing a localization length $\ell = 440d$. Then if the global structure length L is greater than ℓ the regime is localized and it is metallic in the opposite case, whereas if L is similar to ℓ the structure is found in the diffusive regime.

Knowing the average length between impurities is trivial to determine the number of vertices corresponding to the localization length (N_ℓ) using the equation (4.4). For instance, in this case it obtains $N_\ell = 22$. Then, there is a metallic regime for $N << N_\ell$ and a localized regime for $N >> N_\ell$,

$$N_\ell = \frac{\ell}{l_o} \, . \tag{4.4}$$

4.1.2 Conductance

The conductance is the nanowire property that determines the ease of passage of electrons. In other words, the current along the quantum wire. As the same word says, the remarkable feature of the metallic region is a high conductance while in the localized area it vanishes. This behaviour is seen in the Figure 4.2.

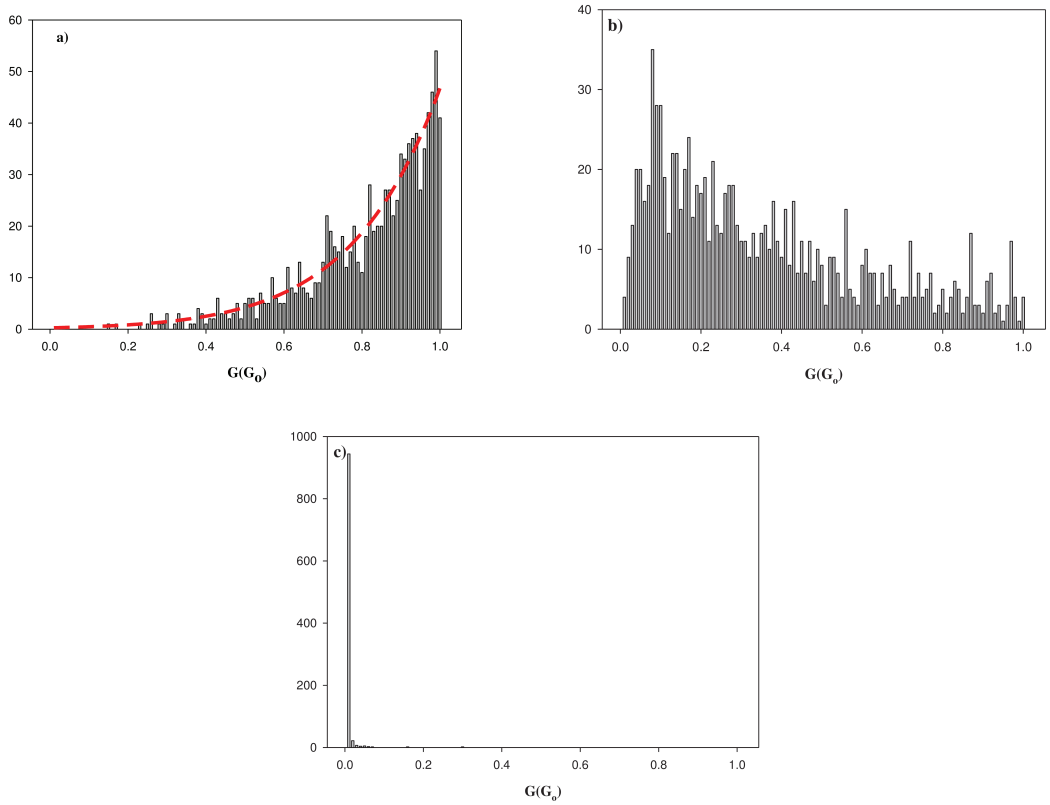

Figure 4.2: Histograms of the conductance in the three regions: metallic (a), diffusive (b) and localized (c). The same parameters of Figure 4.1 have been used. The dashed line for the first panel is a reference to the normal distribution focus on the maximum conductance being limited for the case of only one mode.

For a nanowire with several channels, i.e., several numbers of transversal modes, the transmission can be greater than one, and therefore as it has been explained above there would be a normal distribution of the expected value. In the limit of only one mode the conductance behaviour is the same, although the maximum transmission can only be $\mathcal{T} = 1$ (see Figure 4.2.a). For this reason, the right portion of the normal distribution does not appear. For this instance, the expected value of the conductance is $< G >= 0.8157 G_0$.

Histograms 4.2.b and 4.2.c show the conductance distribution in the diffusive and localized regimes respectively. In the first one, the distribution characterized by the metallic region is broken and transmission value decreases. In the last one, the conductance tends to vanish, obtaining the expected value $< G >= 1.3849 \cdot 10^{-2} G_0$, so the electron transmission does not exist in accordance to the Anderson localization.

4.1.3 Resistance

Conspicuously, the resistance as the equation (4.3) indicates, is the inverse of the conductance. Its behaviour is similar in the three different regions although it has a remarkable difference in the scale (see Figure 4.3).

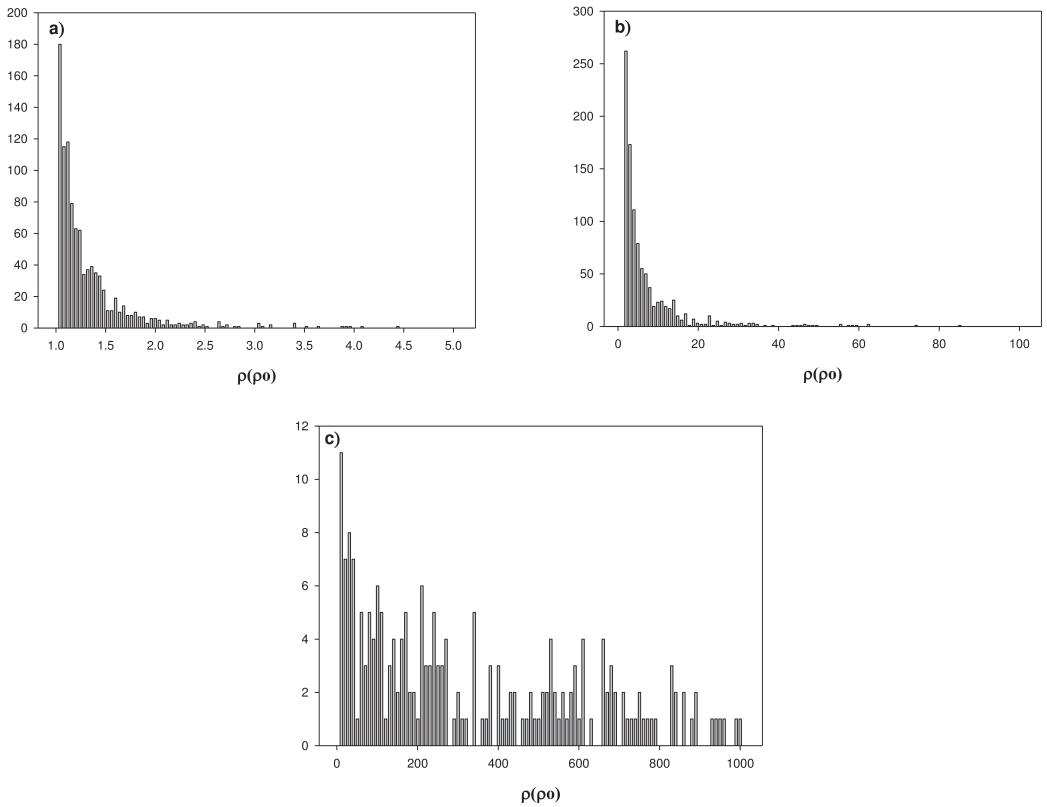

Figure 4.3: Histograms of the resistance in the three regions: metallic (a), diffusive (b) and localized (c). Parameters used are same as Figure 4.1. For the last panel, the resistance value is truncated.

The main problem to compute the resistance is its limit. For the case 4.3.a and 4.3.b the resistance has small values with a stable behaviour. In the last panel, the resistance has higher values and the distribution does not vanish because of the resistance increase exponentially in the localized regime.

The physics of figures 4.2 and 4.3 concur between them. For instance, both panels (c) determine the distribution in the localized region, where the current vanishes, it implies a high resistance and a low conductance.

4.2 Comparison between two systems

Figure 4.4 compares the wire properties between an additional system and the preceding case. This new system is characterized by an average length $l_0 = 50d$ and the rest of the parameters are same as the system in section 4.1. In this section, the behaviour of the conductance and the Lyapunov is compared in the metallic region (left-pair panels) and in the localized regime (right-pair panels), respectively. In the diffusive regime (not shown) the behaviour of these properties lacks a characteristic pattern.

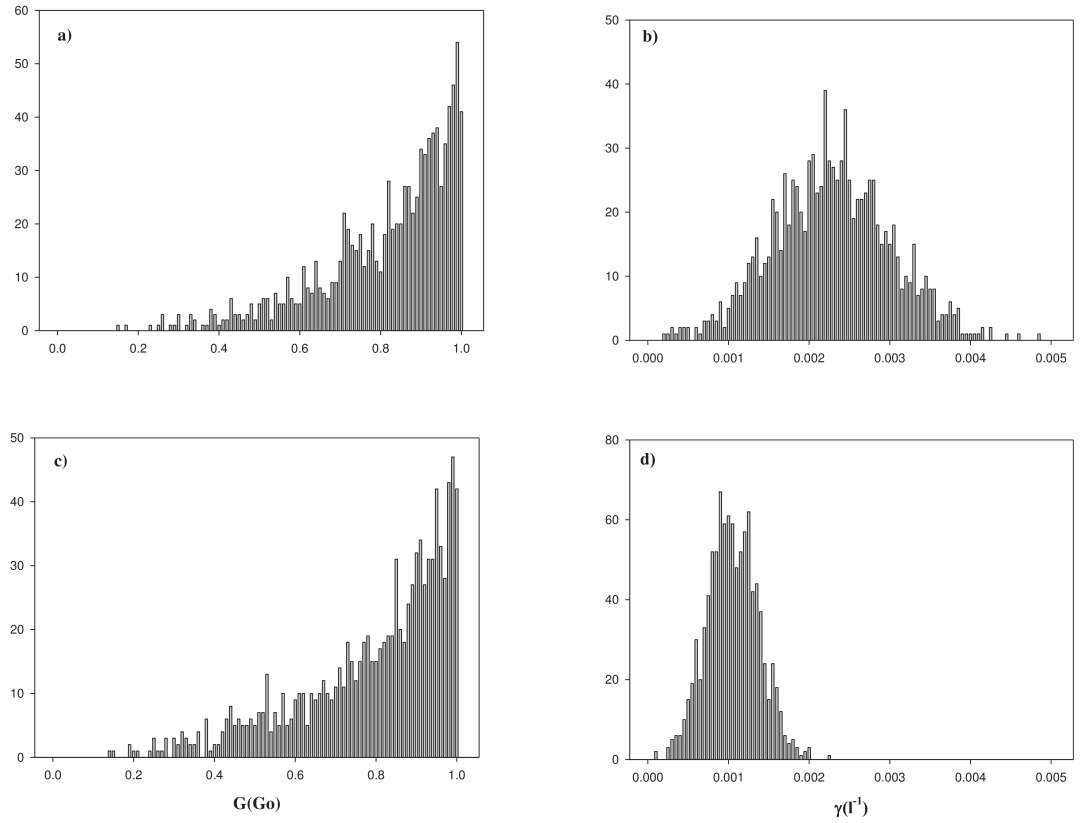

Figure 4.4: Histograms (a) and (b) show the conductance and Lyapunov exponent, respectively, for a system with and average length of the wire $l_0 = 20d$. In the case of a system with $l_0 = 50d$ these histograms are shown in panels (c) and (d).

The conductance always has the same pattern in the metallic area for different systems provided only one transversal mode is active. Although the Lyapunov exponent has the same behaviour indicating the localized regime, each one is focussed on different value. An smaller Lyapunov exponent implies a higher localization length (see table 4.1). Therefore, the Anderson localization is determined by the parameters of the system and in the most general case the localization length depends on l_0, θ_0 and E. In this particular case, it was checked the dependency with the parameter l_0. In addition, in the limit of an infinite length, the quantum wire regulated by this system will always be in the localized regime.

Using the equation (4.4), it is possible to determine the number of vertexes N_ℓ for each system. Although, in the system with $l_0 = 50d$ the localized length is higher than in the system with $l_0 = 20d$, interestingly, the number N_ℓ is almost unchanged. It shows a slight opposite tendency. (table 4.1).

Table 4.1: Results for different systems depends on the average length l_o with the energy $E = 4.94$ and deviation angle $\theta_0 = 1\ rad$. Quantities determined are the conductance (G), the Lyapunov exponent (γ), the localized length (ℓ) and its number of vertex (N_ℓ).

$l_o\ (d)$	$\langle G(G_o)\rangle$	$\langle\gamma(d^{-1})\rangle$	$\langle\ell(d)\rangle$	N_ℓ
20	0.8157	$2.2725 \cdot 10^{-3}$	440.04	22
50	0.7924	$1.0525 \cdot 10^{-3}$	950.12	19

4.3 Dependence with the impurities

The conductance changes with the global length of the system, as it is proportional to the number of vertices it is possible to know how this property depends on it. The table 4.2 shows results of conductance and Lyapunov exponent for a range of vertices. For high number N_v, it can be seen a constant value of γ indicating its size independence previously explained.

Table 4.2: Results for a system with parameters: $l_0 = 20d$, $\theta_0 = 1\ rad$ and $E = 4.94$. The quantities shown are the conductance (G) and the Lyapunov exponent (γ) from a specific number of vertices (N_v).

N_v	$\langle G(G_o)\rangle$	$\langle\gamma(d^{-1})\rangle$
5	0.8157	$1.44 \cdot 10^{-3}$
10	0.6563	$1.71 \cdot 10^{-3}$
15	0.5670	$1.74 \cdot 10^{-3}$
20	0.4728	$1.80 \cdot 10^{-3}$
25	0.4032	$1.95 \cdot 10^{-3}$
50	0.1929	$2.18 \cdot 10^{-3}$
60	0.1557	$2.13 \cdot 10^{-3}$
90	0.0685	$2.28 \cdot 10^{-3}$
150	0.0210	$2.27 \cdot 10^{-3}$
200	0.0138	$2.27 \cdot 10^{-3}$

In accordance with the Anderson localization theory, the conductance shows a lineal and an exponential trend in the metallic and localized regimes, respectively. This phenomenon can be checked in the figure 4.5 that shows the conductance dependence with the number of vertexes. The better portion is identified as the exponential where the conductance tends to vanish. The length belonging to the metallic regime is too small for the studied system.

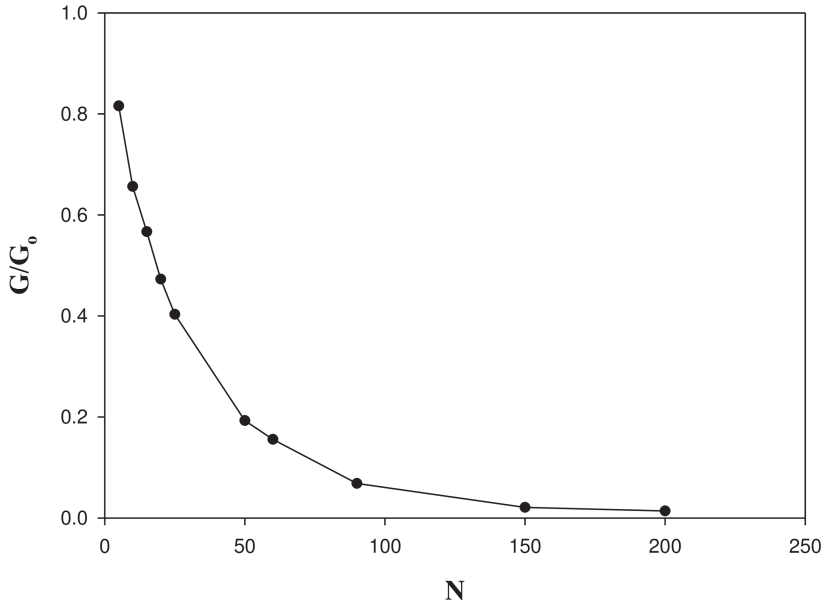

Figure 4.5: Conductance dependence with the number of vertices from the values of the table 4.2.

Conclusions

This research have been focused on the Anderson localization phenomenon, studying the conductance behaviour and the classification of the system in three regimes (metallic, diffusive and localized) depending on the localization length determined from the Lyapunov exponent.

The system studied is a quantum wire made of individual 1D nanowires with a random length linked between them by vertexes with a random angle. Each vertex is treated as a scatterer studied from the scattering theory of circular 2D bend nanowire. The scattering matrix of the vertex is characterized by its simple analytical approximations transforming the problem of a 2D circular bend in a 1D square well potential.

Results of the system determined from the randomness of some parameters agree with the theory explained from the studies of the Anderson localizations and similar statistical studies. For instance, the normal distribution of the conductance in the metallic regime and the Gaussian distribution of the Lyapunov exponent in the localized regime have been tested. In addition, these quantities have been studied for different systems understanding the dependence of the localization length with the system parameters.

This work is the beginning for the study of a nanowire made of quantum wires of random length and linked by a vertex in a random position, where this vertex is treated as a scatterer.

It would be interesting to determine how the localization length varies in a given system when energies span between the first and second transversal mode energies. Some preliminary calculations indicate a non linear dependence.

Evidently, this study is restricted because of the use of approximations in the scattering matrix of a vertex and the limit of only one mode. For a full research the model of coupled channels and spin-orbit interactions should be added.

Bibliography

[1] Guozhong Cao, *Nanostructures & Nanomaterials Synthesis, Properties & Applications*. Imperial College Press, 2004.

[2] G.E. Moore, "Cramming more components onto integrated circuits", *Electronics*, vol. 38, no 8, 1965.

[3] E. Boysen, [online], Nanowires: Uses and Applications of Nanowires, http://www.understandingnano.com/nanowires-applications.html

[4] Thomas Ihn, *Semiconductor Nanostructures quantum states and electronic transport*. Oxford University Press, 2010.

[5] P.W. Anderson, "Absence of diffusion in certain random lattices", *Physical Review*, vol. 109, no 5, pp. 1492-1505, 1958.

[6] L.S. Froufe-Pérez, M. Yépez, A. García-Martín and J.J. Sáenz, "Statistical properties of the conductance of disordered wires: from atomic-scale contacts to macroscopically long nanowires", *Aip Conference Proceedings*, vol. 1319, no 1, 2010.

[7] L.S. Froufe-Pérez, P. García-Mochales, P.A. Serena, P.A. Mello and J.J. Sáenz, "Conductance distributions in quasi-one-dimensional disordered wires", *Physical Review Letters*, vol. 89, no 24, 2002.

[8] A. García-Martín and J.J. Sáenz, "Universal conductance distributions in the crossover between diffusive and localization regimes", *Physical Review Letters*, vol. 87, no 11, 2001.

[9] L. Serra and M.-S. Choi, "Conductance of tubular nanowires with disorder", *The European Physical Journal B*,vol. 71, pp. 97-103, 2009.

[10] K. Flensberg and C.M. Marcus, "Bends in nanotubes allow electric spin control and coupling", *Physical Review B*, vol. 81, 2010.

[11] F. Sols and M. Macucci, "Circular bends in electron waveguides", *Physical Review B*, vol. 41, no 17, 1990.

[12] D.W.L. Sprung, J. Martorell and H. Wu, "Understanding quantum wires with circular bends", *Journal of Applied Physics*, vol. 71, no 1, 1992.

[13] L. Serra and C. Estarellas, "A scattering model of 1D quantum wire regular polugons", *Superlattices and Microstructures*, vol. 83, pp. 184-192, 2015.

[14] H. Jensen and H. Koppe, "Quantum mechanics with constraints", *Annals of Physics*, vol. 63, pp. 586-591, 1971.